Wear resistant all-PE single-component composites via 1D nanostructure formation during melt processing

Timo Hees[1], Fan Zhong[1], Christof Koplin[2], Raimund Jaeger[2,3], Rolf Mülhaupt[1,3]

[1]Freiburg Materials Research Center FMF and Institute for Macromolecular Chemistry, Albert-Ludwigs-University Freiburg, Stefan-Meier-Str. 21, D-79104, Germany

[2]Fraunhofer Institute for Mechanics of Materials IWM, Wöhlerstr. 11, D-79108 Freiburg, Germany

[3]Sustainability Center Freiburg, Ecker-Str. 4, D-79104 Freiburg, Germany

Keywords: Composite, nanofiber, blends, self-reinforcement, wear resistance.

Abstract

Melt-flow-induced crystallization of polyethylene blends having tailored ultrabroad molar mass distribution affords extended-chain ultrahigh molar mass (UHMWPE) nanophases resembling nanofibers which effectively reinforce the polyethylene matrix. Unparalleled by state-of-the-art high density polyethylene (HDPE), the resulting melt-processable "all-polyethylene" single component composites exhibit simultaneously improved wear resistance, toughness, stiffness and strength. Key intermediates are trimodal blends prepared by melt compounding HDPE with bimodal UHMWPE/HDPE wax reactor blends (RB) readily tailored by ethylene polymerization on supported two-site catalysts. Whereas HDPE wax, varied up to 54 wt.-%, serves as processing aid lowering melt viscosity, UHMWPE varied up to 63 wt.-% accounts for improved blend properties. UHMWPE platelet-like nanophase

separate during ethylene polymerization and readily melt during injection molding of RB/HDPE blends producing extended-chain fiber-like UHMWPE nanostructures of 100 nm diameter as shish which nucleate HDPE and HDPE wax crystallization to form shish-kebab-like structures. At 32 wt.-% UHMWPE content shish-kebab-like reinforcing phases account for massive polyethylene self-reinforcement as reflected by improved Young's modulus (+ 420%), tensile strength (+ 740%) and notched Izod impact strength (+ 650%) without impairing HDPE injection molding. All-PE composites exhibit high wear resistance entering ranges typical for polyamide and monomodal UHMWPE which is not processable by injection molding under identical conditions.

Introduction

Hydrocarbon polymers like polyethylene and polypropylene are well known as versatile commodity plastics appearing in daily life applications ranging from packaging, thermal and electrical insulation and textiles to light-weight engineering in automotive and construction industries.[1] Among polyolefins ultrahigh molar mass polyethylene (UHMWPE) with molecular weight exceeding one million g mol^{-1} is well known for exhibiting extraordinary toughness, high strength and outstanding wear resistance.[2] Hence, high performance UHMWPE is used to fabricate ultra-strong fibers, bullet-proof body armor and highly wear resistant components of artificial hips and joints.[2–6] However, increasing polyethylene chain length accounts for massive chain entanglement accompanied by drastic viscosity build-up precluding melt processing of UHMWPE by injection molding, blow molding or extrusion typical for HDPE commodities.[2] Hence manufacturing of high performance UHMWPE is either achieved by gel spinning producing ultra-strong micron-sized extended-chain UHMWPE fibers, UHMWPE powder sintering, special molding processes like ram extrusion or multi-step processing such as lamination of UHMWPE fabrics or hot compaction of

stretched UHMWPE tapes. Aiming at improving HDPE performance it is highly attractive to reinforce HDPE with extended-chain UHMWPE nanofibers to produce all-PE composites via flow-induced oriented crystallization without drastically impairing HDPE injection molding. However, UHMWPE nanofibers are not available and would require special handling and safety procedures. Particularly dispersion of nanophase-separated UHMWPE is essential to increase UHMWPE content without encountering massive entanglement paralleled by intolerably high melt viscosity. The basic concept of single-component polymer composites, also being referred to as all-polymer composites, wherein both matrix and reinforcing phase are made from the same polymer, was pioneered by *Porter et al.*[7,8] Progress made in the development of self-reinforced all-polymer composites was reviewed by Kmetty, Bárány and Karger-Kocsis.[9] According to Keller the presence of high molar mass polyethylene is essential for achieving flow induced coil-stretch transition by preventing relaxation when surpassing a critical molar mass.[10] In the past many studies relating to shish-kebab fiber reinforced polyethylene employed solution blends and special processing such as compression molding, hot compaction and drawing, since classical HDPE injection molding failed to tolerate high amounts of UHMWPE.[11–16] As verified by *Boscoletto et al.*, in simple melt-mixing of UHMWPE with HDPE less than 3 wt.-% UHMWPE is dissolved.[12] Moreover, it should be noted that commercially available micron-sized UHMWPE does not fully melt during short hold-up times typical for HDPE melt processing and is only useful as micron-sized filler. Melt compounding of HDPE with pre-fabricated UHMWPE nanoparticles would be rather problematic owing to emission problems and severe explosion hazards encountered when handling sub-micron organic electrically insulating particles during conventional polymer processing. As a consequence, most state-of-the-art bimodal HDPE reactor blends, produced in cascade reactors, incorporate minute amounts of UHMWPE serving as tie molecule bonding together HDPE crystallites, thus significantly enhancing fatigue resistance of extruded HDPE pipes.[17]

At the beginning of the 21st century the discovery of robust supported multisite catalysts for reactor blend (RB) formation has enabled unprecedented tailoring of ultrabroad polyethylene molar mass distributions in conjunction with facile dispersion of much larger amounts of nanophase-separated disentangled UHMWPE during ethylene polymerization without adversely affecting HDPE injection molding.[1] The molar ratio of different catalytic sites which independently produce HDPE, UHMWPE, and if desired also HDPE wax, on the same catalyst support governs the weight ratio of polyethylenes with vastly different chain lengths without changing the average molar mass of the individual fractions. Even unprecedented ultrabroad bimodal nanostructured polyethylene RBs containing UHMWPE 1D nanostructures embedded in HDPE wax became feasible in industrial ethylene polymerization processes typical for HDPE commodity production without encountering reactor fouling.[18] For the first time more than 10 wt.-% nanophase-separated UHMWPE was dispersed in HDPE without impairing injection molding typical for HDPE commodities in the absence of UHMWPE.[18–24] Unlike micron-sized UHMWPE, as verified by DSC, X-ray diffraction and electron microscopy, UHMWPE nanostructures readily melt during injection molding to form extended-chain UHMWPE nanofibers by flow-induced crystallization. The resulting extended-chain UHMWPE 1D nanostructures serve as shish nucleating crystallization of HDPE and HDPE wax to produce kebab structures. It was shown that the UHMWPE 1D nanostructures have average diameter of 80 nm.[25] The resulting shish-kebab polyethylene phases reinforce the polyethylene matrix accounting for massive self-reinforcement as reflected by simultaneously improved stiffness, strength and toughness. In order to further enhance self-reinforcement by raising the UHMWPE content ultra-low molar mass HDPE wax was incorporated serving as processing aid and lubricant lowering melt viscosity at higher UMHWPE content.[19,20] Since HDPE wax is incorporated into kebab structures large amounts of HDPE wax is tolerated in melt processing without encountering massive emission problems typical for HDPE/HDPE wax melt compounds in the absence of UHMWPE

nanostructures. As an alternative route towards all-PE single-component composites polyethylene RBs with ultrabroad bimodal molar mass distributions, readily tailored by ethylene polymerization on two-site catalysts, are employed as additives for HDPE melt processing in order to tailor trimodal molar mass distributions without requiring modifications of the polymerization processes producing HDPE commodities.[23] Unlike all-PE composites prepared by ethylene polymerization on three-site catalysts, in which catalyst composition governs all-PE composite performance, the reactor blend additive approach enables to control all-PE single-component composite properties via the RB content. Albeit significant progress has been made in all-PE composite development exploiting both ethylene polymerization on three-site catalyst and melt compounding of HDPE with bimodal reactor blend additive little is known concerning the wear resistance of all-PE single-component composites. Herein we examine how to tailor RB additives and nanostructured polyethylene with ultrabroad trimodal molar mass distributions in order to simultaneous increase wear resistance, stiffness, strength and toughness of all-PE composites. Special focus is placed upon injection molding of all-PE composite exhibiting high wear resistance similar to UHMWPE without impairing facile melt processability typical for HDPE commodities. The ultimate goal is to develop melt-processable all-PE single composite materials by converting HDPE commodities into high performance engineering thermoplastics self-reinforced by in-situ UHMWPE 1D nanostructure reinforcement without sacrificing facile processing in conjunction with attractive cost, resource, eco and energy efficiency typical for polyolefin commodities.

Experimental section

MATERIALS AND METHODS

All polymerizations and catalyst preparation steps involving air- or moisture-sensitive substances were carried out under a dry argon atmosphere and a glovebox (MB Braun MB

150-G-II). Ethylene (3.0) and Argon (5.0) were purchased from Messer Griesheim and used without further purification. Toluene (anhydrous, Sigma-Aldrich), *n*-heptane (anhydrous, Merck) were purchased and further purified with a Vacuum Atmospheres Co. solvent purifier. Methylaluminoxane (10 wt.-% in toluene), trimethylaluminum (TMA, 2 M in n-heptane) and triisobutylaluminum (TiBAl, 1 M in n-hexane) were purchased from Sigma-Aldrich. Mesoporous silica (silica nanofoam, NF70) exhibiting a pore diameter of 70 nm and specific surface of 790 $m^2 g^{-1}$ was synthesized in our group according to previously reported procedures.[18,22,43] 2,6-Bis-[1-(2,6-dimethylphenylimino)ethyl] pyridine chromium (III) trichloride (CrBIP) was synthesized according to a literature procedure.[44] [η^5-3,4,5-trimethyl-1-(8-quinolyl)-2 trimethylsilyl-cyclopentadienyl-chromium dichloride (CrQCp) was synthesized and kindly supplied by the group of Enders (University of Heidelberg).[45,46] Hostalen GC7260 (M_w = 77 kg mol^{-1}, Mw/Mn = 4.6), which was used as bulk material and HDPE benchmark was supplied by Lyondellbasell. The UHMWPE reference (GUR 4120) and PA46 (Stanyl) was supplied by Celanese and DSM, respectively.

CATALYST PREPARATION AND ETHYLENE POLYMERIZATION

The mesoporous silica catalyst support (NF70) was dried in a Schlenk-tube in high-vacuum (10^{-3} bar) at 160 °C for 14 h. 20 mL of toluene were added and the suspension was sonicated for 10 min. After adding of the calculated amount of MAO (Al : Cr = 300 : 1), the mixture was stirred for 30 min and sonicated for 5 min. After sedimentation, the MAO-treated catalyst support was washed with dry toluene by removal and exchange of the supernatant. CrBIP was dissolved in toluene (0.2 mg mL^{-1}), pretreated with TMA (10 equiv.) and added by syringe. After stirring for 5 min, CrQCp in toluene (0.2 mg mL^{-1}) was also added and the mixture was stirred again for 5 min. After sedimentation, the activated catalyst was collected in n-heptane (20 mL), transferred into the reactor and the polymerization was started. Ethylene polymerizations were carried out in a 2.6 L steel reactor (HITEC ZANG) equipped with a mechanical stirrer, thermostat and a software interface. Therefore, the reactor was heated in

high-vacuum at 90 °C for 2 h, pre-filled with *n*-heptane (580 mL) and TiBAl (3 mL, 1 M in *n*-hexane) and was saturated with ethylene (5 bar). After transferring the prepared catalyst into the reactor, the polymerization was proceeded at 40 °C, an ethylene pressure of 5 bar and stirring speed of 200 rpm for 120 min. The polymer was stabilized with BHT (2,6-Di-*tert*-butyl-4-methylphenol) in methanol, filtered and dried under reduced pressure at 60 °C to constant weight.

RB CHARACTERIZATION

Thermal characterization was conducted by differential scanning calorimetry (DSC) by using a DSC 204 F1 Phoenix from NETSCH. Molecular weight (M_w) and Molecular weight distributions (MWD) were determined with a PL-220 high temperature gel permeation chromatograph (HT-GPC, Agilent) equipped with three PLGel Olexis columns and a triple-detection system (differential refractive index detector, differential viscometer 210 R (Viscotek), low-angle lightscattering detector). The columns were calibrated using 12 polystyrene samples with narrow MWDs. Measurements were operated at 160 °C in 1,2,4-trichlorbenzene (stabilized with 0.2 wt.-% 2,6-di-tert-butyl-(4-methylphenol)) at flow-rates of 1.0 mL min^{-1}. Morphological investigations of nanostructure formation were performed using a scanning electron microscope Amray 1810.

POLYMER MELT PROCESSING

Typically, HDPE pellets were milled (Hellweg Maschinenbau GmbH & Co. KG; grit size ≤1 mm) prior to physical mixing and melt compounding with the reactor blend powders. The bimodal reactor blend powders (RB33, RB50 and RB63) were suspended in acetone and stabilized with 0.2 wt.-% of Irganox 1010 and Irgafos P168 (1:1). The desired amount of HDPE (Hostalen GC7260) was added prior to solvent removal under reduced pressure and drying of the polymer in vacuum at 65 °C to constant weight. Melt processing was performed with a co-rotating twin-screw micro compounder Xplore (DSM, Heerlen, Netherlands) at 200 °C and 120 rpm for 2 min and subsequently injection molded into tensile and impact

strength test specimens by an injection molding device Xplore (DSM, Heerlen, Netherlands) at 60 °C mold temperature and injection pressure of 9 bar.

MECHANICAL AND TRIBOLOGICAL CHARACTERIZATION

Mechanical properties like Young's Modulus, tensile strength or notched impact strength were determined with a Zwick model Z005 according to DIN-EN-ISO 527 (tensile test method 5A) and a Zwick pendulum according to DIN-EN-ISO 180 (Izod method), respectively. The tribological behavior of the materials was investigated with a custom-made "Pin on Ring"-Tribometer (1 rpm, 0.27 m s^{-1}, 3 MPa pressure, ment ratio of polymer to steel: 1/270, Pin: rectangular shaped polymer specimen, ring: dry steel disc (AS6590, hardened, polished) with R_a: 0.2-0.3 µm, R_z: 2-3 µm, $R_{ku:}$ 3.5-5.5, R_{pc}: ~200 cm^{-1}, surface energy: $\sigma_{dispersive}$ (28 mN/m), σ_{polar} (7 mN/m), environment: RT, 30-40 % rel. humidity). Specimens were cut from the tapered section of injection-molded tensile test specimens where a higher translucency of the specimen indicated a higher preferential orientation of the polymer chains. The specimens were oriented such that the preferential orientation of the polymer chains was perpendicular to the surface of the frictional partner. All measurements were carried out with a new steel ring in order to provide identical conditions wherein each polymer pin came initially in contact with a "virgin" steel surface. The wear experiments were repeated three times per material.

Results and Discussion

TAILORING ALL-PE COMPOSITES

Whereas most state-of-the-art injection-moldable all-PE single-component composites have been tailored by ethylene polymerization on specifically designed supported three-site catalyst we employ the additive route blending together HDPE commodity resins with bimodal reactor blends (RB) containing nanophase separated UHMWPE embedded in HDPE wax.[23] Addition

of RB additives to HDPE melts does not require modification of the catalytic process established for manufacturing of HDPE commodities. Key feature of this process is flow-induced oriented UHMWPE crystallization producing disentangled extended-chain UHMWPE 1D nanostructures resembling ultrastrong UHMWPE nanofibers which reinforce the HDPE matrix. Preferably RB comprises nanophase separated disentangled UHMWPE dispersed in HDPE wax which serves as lubricant and processing aid lowering HDPE melt viscosity and enabling melt processing in the presence of high UHMWPE contents without impairing HDPE injection molding and extrusion. The ratio of UHMWPE/HDPE wax is set by the molar ratio of two catalytic sites producing UHMWPE and HDPE wax on the same catalyst support. Owing to the close proximity of the two sites, it is possible to form nanophase separated RBs which are not feasible by conventional melt compounding of HDPE wax with UHMWPE. The UHMWPE content of all-PE composites at constant UHMWPE/HDPE wax ratio is governed by the RB addition during melt compounding. As is illustrated in **Scheme 1** RB contains nanoplatelet-like UHMWPE which is dispersed in HDPE wax and readily melts forming disentangled extended-chain UHMWPE 1D nanostructures resembling nanofibers which nucleate HDPE and HDPE wax crystallization producing shish-kebab-fiber-like nanostructures as reinforcing phases.

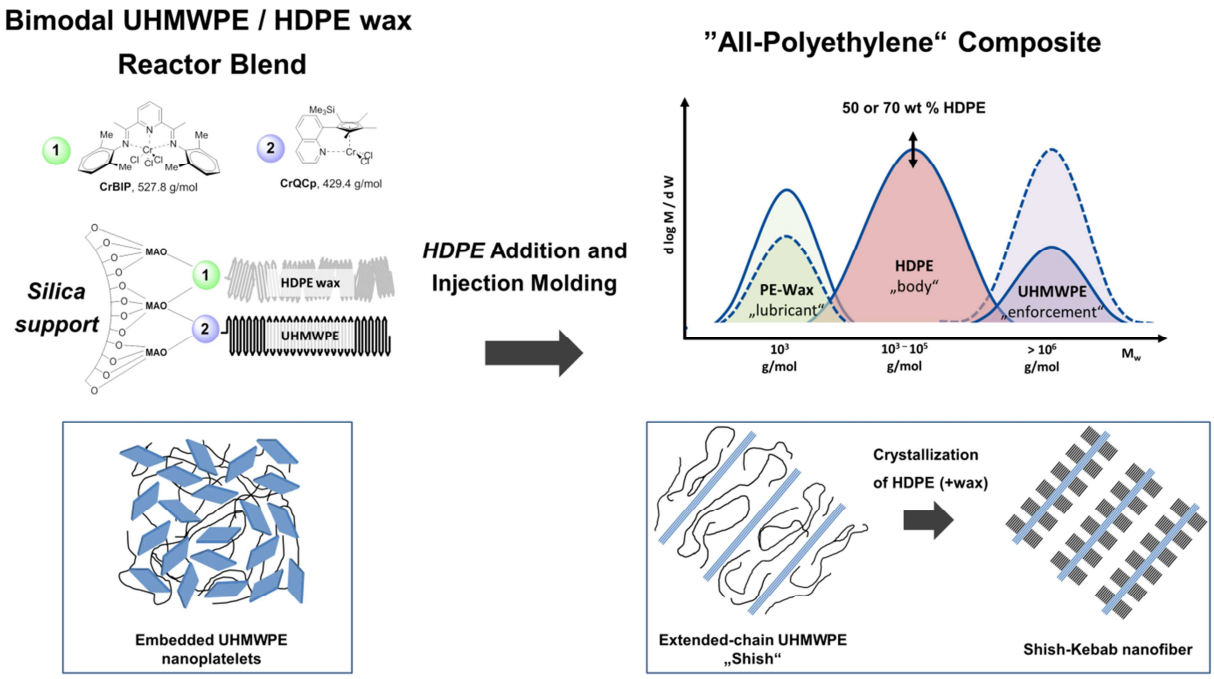

Scheme 1: Melt compounding of HDPE with various bimodal UHMWPE/HDPE wax reactor blends to produce "all-polyethylene" single-component composites reinforced with extended-chain UHMWPE 1D nanostructures resembling shish-kebab nanofibers. The RB addition to HDPE enables tailoring of trimodal polyethylene with variable UHMWPE content at constant UHMWPE/HDPE wax weight ratio.

Typically, the RB additives were tailored by ethylene polymerization on methylaluminoxane (MAO)-activated supported two-site catalysts combining 2,6-bis-[1-(2,6-dimethylphenylimino)ethyl] pyridine chromium (III) trichloride (CrBIP), producing HDPE wax (10^3 g mol^{-1}) and [η^5-3,4,5-trimethyl-1-(8-quinolyl)-2 trimethylsilyl-cyclopentadienyl-chromium dichloride (CrQCp), producing UHMWPE (2×10^6 g mol^{-1}). Both CrBIP and CrQCp were co-immobilized on MAO-tethered mesoporous silica having 70 nm pore size. Varying the CrBIP/CrQCp molar ratio enabled precise control of the HDPE wax / UHMWPE weight ratio of the RB additive. For instance, tuning CrBIP/CrQCp molar ratio from 9.5 to 4.7 and 3.2 raised the UHMWPE content of the RB additive from 33 to 50 and 63 wt.-% (see **Table 1** and also **Figure 1**). The sample identification RB33 denotes that the reactor blend RB contained 33 wt.-% UHMWPE. From the GPC traces in Figure 1 is apparent that variation of the CrBIP/CrQCp molar ratio precisely controlled the HDPE wax/UHMWPE weight ratio

but did not affect the average molar mass of either HDPE wax or UHMWPE. All RB samples had ultrabroad bimodal molar mass distribution with M_w/M_n varying between 500 and 1050.

Table 1: RB prepared by ethylene polymerizations on silica-supported two-site chromium catalysts combining CrBIP and CrQCp co-immobilized on the NF70 silica support.

entry	CrBIP/CrQCp [mol/mol]	Yield [g]	HDPE wax[a] [wt.-%]	UHMWPE[a] [wt.-%]	T_m[b] [°C]	ΔHc[b] [J g^{-1}]	M_w[a] [kg mol^{-1}]	M_w/M_n[a]
RB33	9.5	282	54	33	130	154	1220	1000
RB50	4.7	319	35	50	132	163	1690	1050
RB63	3.2	318	17	63	137	157	1790	500

Further conditions: m_{NF70}= 200 mg, $V_{heptane}$= 600 ml, $p_{Ethylene}$= 5 bar, V_{TiBAl} T_{pol}= 40 °C, t_{pol}= 120 min [a] Determined by high-temperature gel permeation chromatography (HT-GPC). [b] First DSC heating cycle.

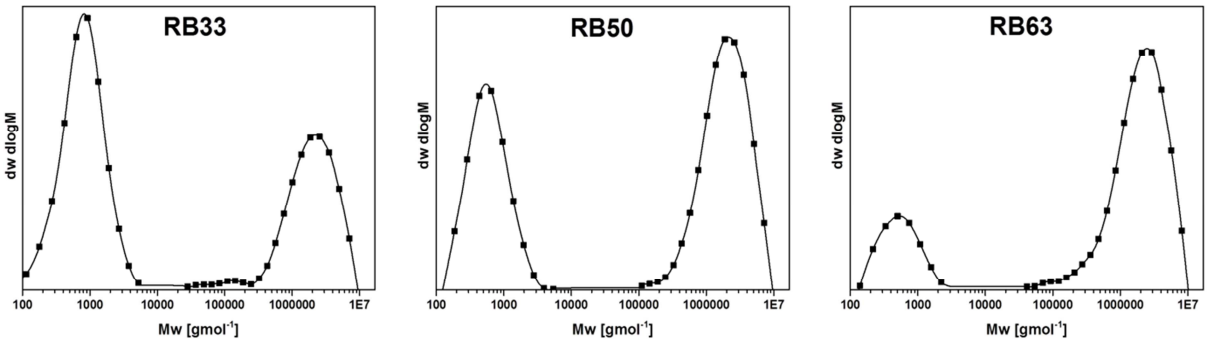

Figure 1: Molar mass distributions of RB33, RB50 and RB63 as determined by HT-GPC.

In order to investigate the influence of HDPE wax, HDPE and UHMWPE on mechanical, morphological and tribological properties, the bimodal RBs with different UHMWPE / HDPE wax ratios were melt compounded with intermediate molar mass HDPE using a twin-screw microcompounder at 200 °C and 120 rpm prior to injection molding of the resulting trimodal all-PE composite. Sample identification xxRByy denotes "xx" as wt.-% RB added to HDPE whereas RByy specifies the type of bimodal reactor blend as listed in Table 1. Although the total UHMWPE contents of the HDPE/RB blends were in the range of 20-30 wt.-% (see Table 2), all samples were readily melt-processable by injection molding at 200°C

using the same parameters typical for the injection molding of neat HDPE. Opposite to HDPE/HDPE wax blends in the absence of nanophase-separated UHMWPE no HDPE wax emission and odor problems were encountered in the presence of UHMWPE owing HDPE wax crystallization onto UHMWPE shish forming kebab structures. In accord with earlier observations[20], co-supporting of CrQCp with other (post-)metallocenes afforded nanophase separation as reflected by the incorporation of platelet-like UHMWPE nanostructures which prevented entanglements of UHMWPE chains. By means of melt compounding HDPE with various amounts of the three different RB additives the HDPE content was varied between 59 to 100 %, the HDPE wax content from 0 to 16 wt.-% and the UHMWPE content from 0 to 32 wt.-%. As schematically displayed in Scheme 1, this additive strategy involving melt compounding of HDPE with RB additives enables to independently vary UHMWPE / HDPE and UHMWPE / HDPE wax ratios.

Table 2: Compositions of all-PE composites prepared by melt blending HDPE with RB containing HDPE wax and UHMWPE. .

entry	HDPE wax [wt.-%]	HDPE[a] [wt.-%]	UHMWPE [wt.-%]
HDPE	0	100	0
30RB33	16	74	10
30RB50	11	74	15
30RB63	5	76	19
50RB50	18	57	25
50RB63	9	59	32

[a] Includes Hostalen GC7260 and high molecular weight polyethylene below the range of 10^6 g mol^{-1}.

MECHANICAL PROPERTIES

The mechanical properties of all-PE composites as a function of UHMWPE and HDPE wax contents are listed in **Table 3** and displayed in **Figure 2**. Clearly the toughness / stiffness / strength balance significantly increased with increasing UHMWPE content. As compared to HDPE, the all-PE composite 50RB63, containing 50 wt.-% RB50

equivalent to 32 wt.-% total UHMWPE content, exhibited high Young's modulus of 4.8 GPa (+ 420 %), tensile strength of 201 MPa (+ 720 %) and notched Izod impact strength of 34 KJ/m^2 (+ 650 %).

Table 3: Mechanical properties of all-PE single-component composites as a function of HDPE wax and UHMWPE content.

entry	HDPE wax (wt.-%) / UHMWPE (wt.-%)	Young's Modulus[a] [GPa]	Tensile strength[a] [MPa]	Notched Izod impact strength[b] [KJ/m2]
HDPE	-	0.9 ± 0.05	24 ± 1	5 ± 1
30RB33	16 wt.-% / 10 wt.-%	2.4 ± 0.1	97 ± 4	20 ± 2
30RB50	11 wt.-% / 15 wt.-%	2.8 ± 0.4	117 ± 4	25 ± 2
30RB63	5 wt.-% / 19 wt.-%	3.8 ± 0.5	138 ± 5	28 ± 1
50RB50	18 wt.-% / 25 wt.-%	3.2 ± 0.3	142 ± 4	23 ± 2
50RB63	9 wt.-% / 32 wt.-%	4.8 ± 0.5	201 ± 16	34 ± 4

[a] Determined via tensile testing with a Zwick model Z005 according to DIN-EN-ISO 527 (5A) and [b] a Zwick pendulum according to DIN-EN-ISO 180 (Izod method).

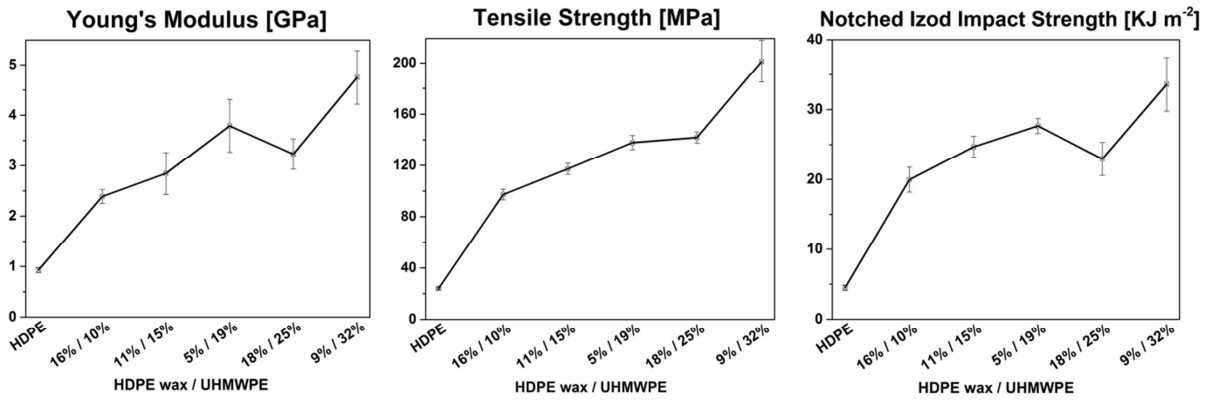

Figure 2: Young's modulus (left), tensile strength (middle) and notched Izod impact strength as a function of HDPE wax and UHMWPE content.

In order to verify the in-situ formation of shish-kebab reinforcing phases comprising extended-chain UHMWPE shish and HDPE/HDPE wax kebab the all-PE composites were analyzed by means of Differential Scanning Calorimetry (DSC) and Scanning Electron Microscopy (SEM). Since extended-chain PE fibers result from flow-induced crystallization all samples were taken from the mid sections of the tensile bars.[19] Evidence of different

crystalline phases is clearly visible by comparing the first and second DSC heating cycles (**Figure 3**). The second higher melting temperature (>140 °C) exclusively appeared during the first heating cycle, whereas no such transition was detected in the second cycle. Obviously extended-chain polyethylene was only formed during injection molding owing to flow-induced crystallization whereas crystallization from melts without extensional flow failed to afford extended-chain polyethylene crystals. This is in accord with previous observations.[26,27]

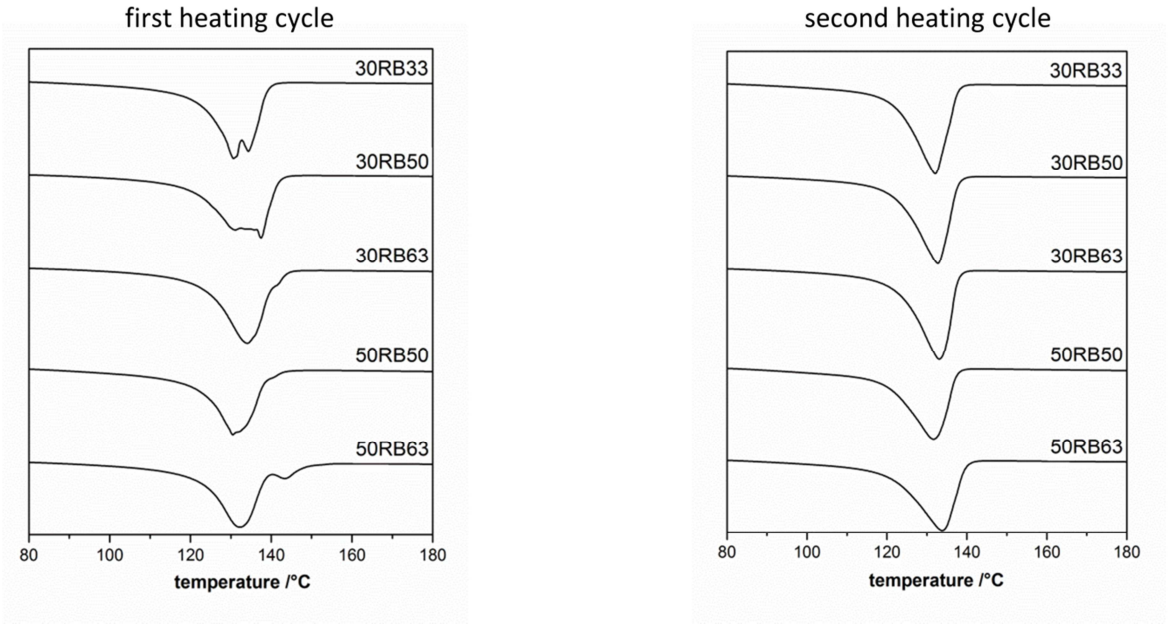

Figure 3: DSC traces of first heating cycle (left) and second heating cycle (right) of injection-molded all-PE composites. The second melting temperature or shoulders, respectively well above 133 °C indicate the presence of extended chain polyethylene crystals.

Shish-kebab reinforcing phases were detected by SEM after etching the samples with hot xylene at 130 °C thus removing soluble amorphous HDPE as well as predominantly low molar mass PE fractions. From **Figure 4** it is apparent that all-PE composites contained shish-kebab structures aligned in flow direction. Sample etching was more efficient in the presence of high amount of wax (see all-PE composite 30B33 in Figure 4). At high UHMWPE content and low HDPE wax content (see sample 30RB63 in Figure 4) UHMWPE platelets were visible owing to incomplete transformation into extended-chain polyethylene structures at low content of HDPE wax which serves as processing aid lowering melt viscosity.

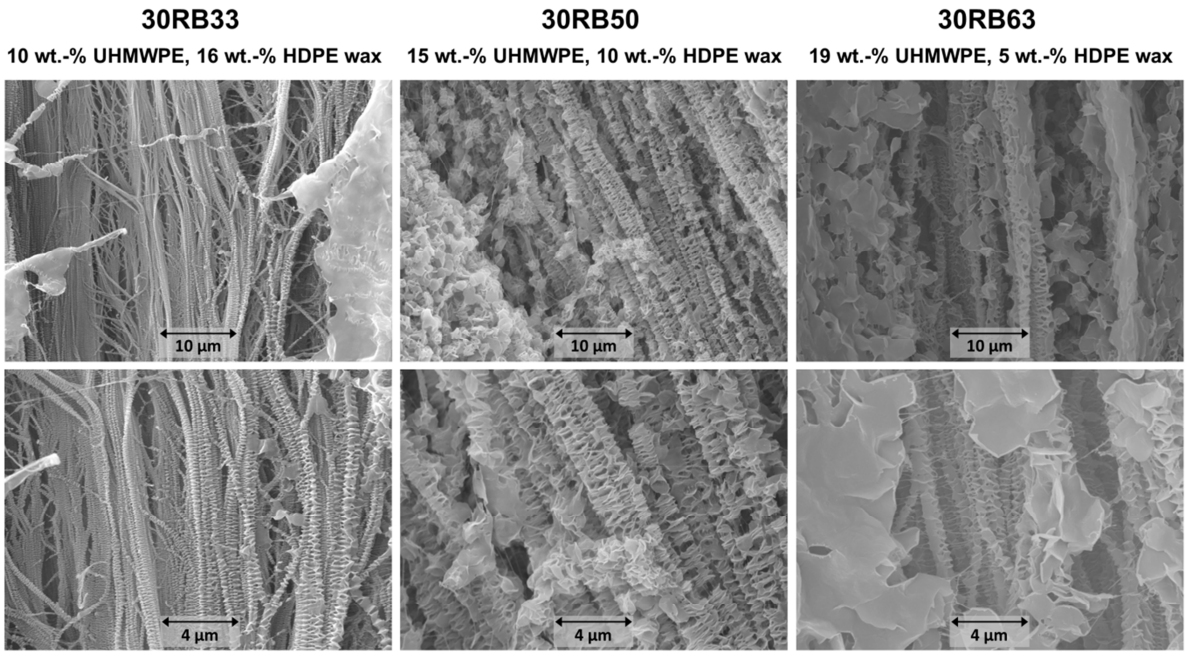

Figure 4: SEM images of injection-molded all-PE composite tensile bars after etching with hot xylene at 130 °C showing shish-kebab fiber structures oriented in flow direction during injection molding.

When samples were annealed at 137 °C below the melting temperature of extended-chain UHMWPE followed by quenching in liquid nitrogen crystallization of HDPE and HDPE wax as well as shish-kebab structure formation were prevented. As verified via SEM (Figure 5) this enables the complete removal of amorphous HDPE with hot xylene at 130 °C and imaging of UHMWPE shish which had an average diameter of 100 nm.

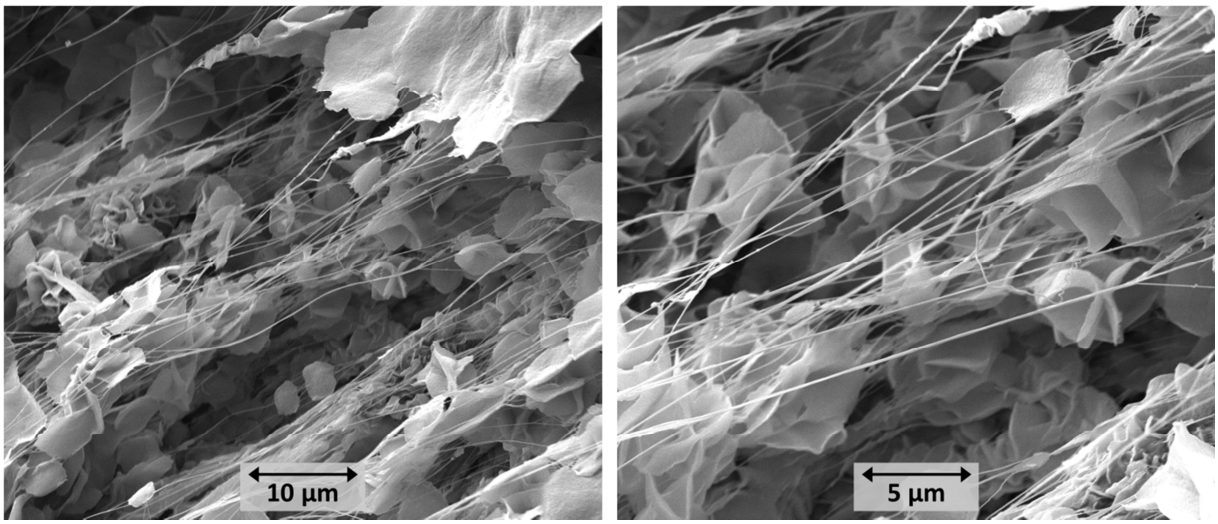

Figure 5: SEM observation of extended-chain UHMWPE 1D nanostructures of 100 nm diameter after annealing of tensile test bars (50RB50) at 137 °C and subsequent extraction of HDPE and HDPE wax fractions with hot xylene.

TRIBOLGICAL CHARACTERIZATION OF ALL-PE COMPOSITES

The interaction of the asperities of the frictional partner with the polymer surface gives a significant contribution to the wear a polymer experiences in the sliding contact with the partner. Depending on the shape of the asperities (in particular the angle of action), the adhesive interaction of the system and the mechanical characteristics of the polymer (e.g. the tensile strength and the failure strain), the interaction between polymer surface and frictional partner can vary from "ironing" over "ductile ploughing" to "brittle machining".[28–31] Since the mechanical characteristics of the polymer can change due to local frictional heating and the rough surface of the frictional partner can be altered by the transfer of a thin polymer layer, wear of polymers is a complex and often time-dependent phenomenon which requires a systemic approach.[32–37] A specific run-in behavior has to be passed before stable and comparable wear rates and friction forces can be estimated.

Polyolefins have a good wear resistance in comparison to other thermoplastics[38,39] but with the exception of UHMWPE[40] they show lower wear resistance as compared to engineering thermoplastics which are typically used in applications where an elevated tribological loading occurs. The comparatively low melting point of polyolefins prohibits their use in high temperature applications or loading situations where a significant frictional heating is expected.[41] In addition, HDPE has a lower Young's-modulus, lower tensile strength and microhardness in comparison to technical polymer composites used in tribological applications. Since mechanical properties of all-polyethylene composites are drastically improved with respect to HDPE, one would also expect an improved wear resistance. In related tests *Zhang et al.* investigated the tribological properties of UHMWPE / HDPE blends processed by different methods and confirmed enhanced wear properties for those samples having better mechanical properties.[42] Furthermore, the HDPE wax fraction could lead to lubricating effects which reduces the wear of the polymer. When testing the polyolefin

composites, three different specimen orientations with respect to the frictional partner are possible: the rectangular blocks can be oriented such that the preferential orientation of the polymer chain is parallel or perpendicular to the frictional surface (see **Scheme 2**). If the orientation is parallel to the surface it can be parallel or perpendicular to the motion. In orientation parallel to the surface the increasing wear depth shows a transition from a skin to a core behavior, on the contrary the orientation perpendicular to the surface averages this transition. If the chains are oriented parallel to the surface and the motion, the shear forces have to be carried by the polymer fibrils and the amorphous interface in which the fibrils are embedded. Initial wear tests with this orientation resulted in high wear rates where the wear rate significantly increased with increasing UHMWPE content of the specimens. Since the end of the fibrils cannot be "clamped" in the sample holder, we observed presumably a rapid shear-failure of the weak amorphous interface between the fibrils. Layers of the rectangular block specimens were sheared-off under the tribological loading. As a consequence, the wear tests were carried out with the polymer fibrils oriented perpendicular to the steel ring and clamped in the specimen holder. A smooth wear surface of the rectangular shaped specimens was observed, indicating a complete contact of the rectangular block specimens with the steel ring.

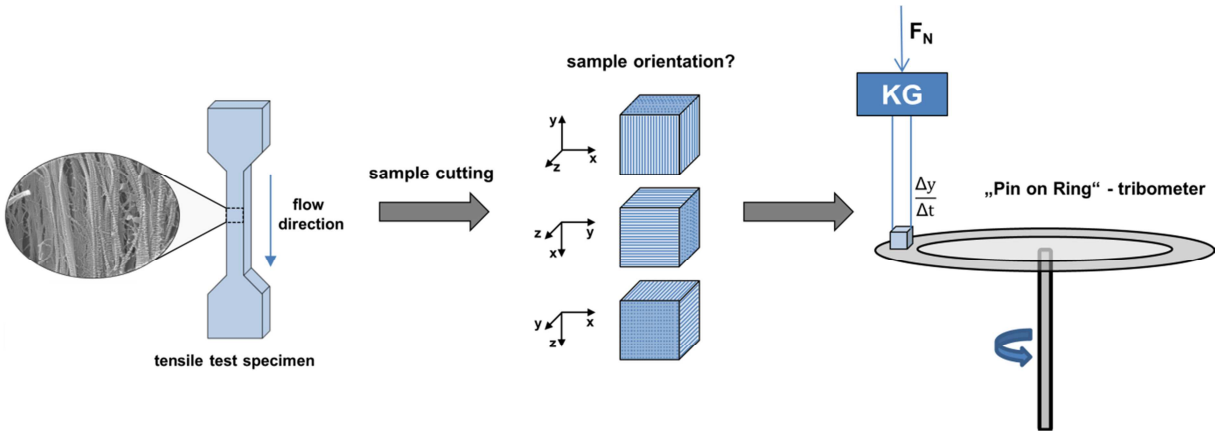

Scheme 2: Tribological investigation of multimodal RB and references with a „Pin on Ring"-tribometer. Samples were taken from the oriented zone of tensile test bars.

In addition to the reactor blend series RB33, RB50 and RB63 which were mechanically characterized in the first part, another bimodal UHMWPE / HDPE wax reactor blend containing 40 wt.-% UHMWPE (RB40) was melt blended with HDPE and included into the wear tests which are summarized in Table 4. The mechanical and morphological characterization of tailored all-PE composites containing RB40 was published previously.[25] Also neat HDPE, compression molded unimodal UHMWPE reference samples and polyamide (PA46) which is frequently used as polymer component in technical composites for tribological applications were tested (see Table 4 and Figure 6).

Table 4: Wear rates in $\mu m\, h^{-1}$ and coefficient of friction as determined by "pin on ring" measurements.

sample	wear rate [$\mu m\, h^{-1}$]		μ	
HDPE	16.0	±3.7	0.21	±0.06
UHMWPE	2.3	±1.6	0.27	±0.09
PA46*	2.3	n.d.	0.23	n.d.
30RB33	4.9	±3.3	0.16	±0.03
30RB50	9.3	±2.6	0.21	±0.06
30RB63	4.1	±3.4	0.14	±0.07
50RB50	6.0	±5.0	0.13	±0.06
50RB63	2.4	±0.7	0.15	±0.02
10RB40	18.9	±7.6	0.17	±0.01
20RB40	9.6	±1.3	0.18	±0.03
30RB40	5.6	±1.5	0.17	±0.02
50RB40	6.2	±0.8	0.21	±0.02
100RB40	5.1	±0.3	0.18	±0.02

*Polyamide sample was only measured once. Further conditions: 1 rpm, 0.27 $m\, s^{-1}$, 3 MPa pressure, Ra: 0.2-0.3 µm, Rz: 2-3 µm, Rku: 3.5-5.5, Rpc: ~200 cm^{-1}, surface energy: $\sigma_{dispersive}$ (28 $mN\, m^{-1}$), σ_{polar} (7 $mN\, m^{-1}$).

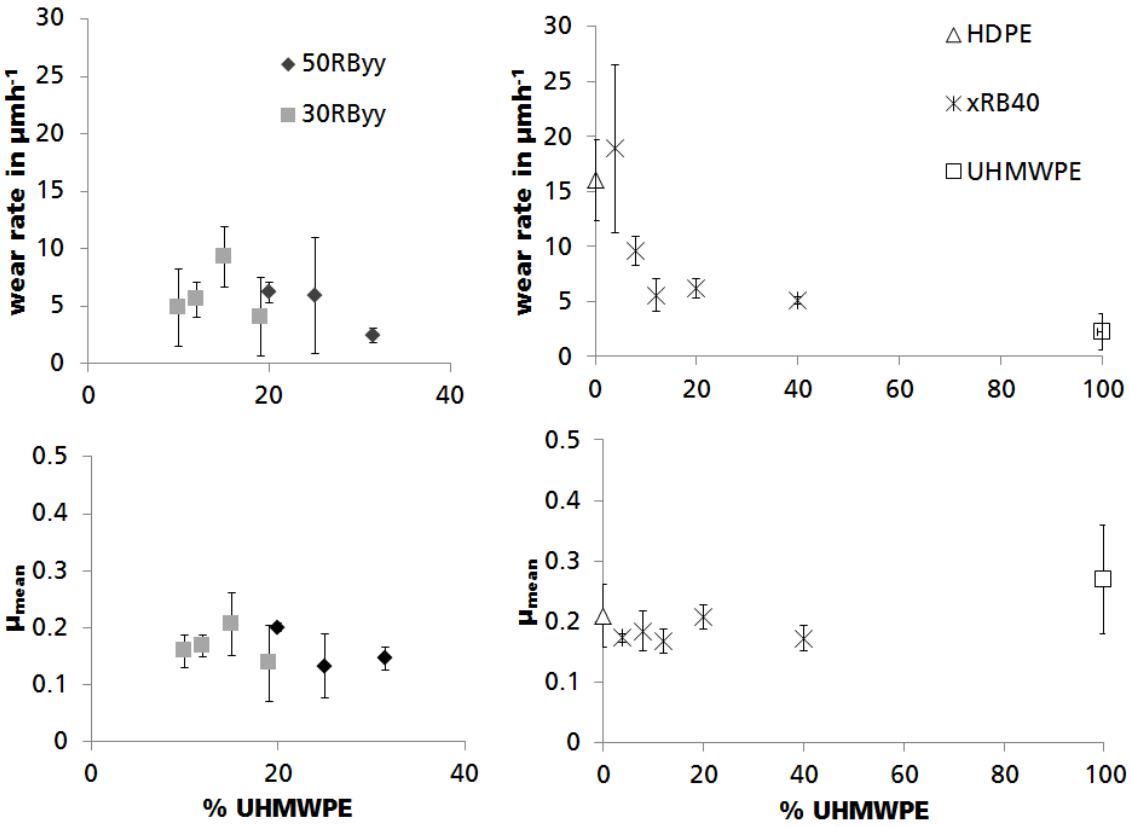

Figure 6: Wear rate (above) and coefficient of friction (below) as a function of UHMWPE content.

The average duration of the run-in period was 12 h and the initial mean wear was 200 µm. The wear rate was determined after the linear relation between wear and time occurred, which resulted in overall gliding times between 18 h up to 2 days. The tribological measurements were repeated three times for each sample composition. While the UHMWPE reference showed a ten times lower wear rate in comparison to the HDPE sample, all-PE composites with even small amounts of HDPE wax and UHMWPE show a significantly improved wear resistance compared to HDPE. By increasing the amount of UHMWPE in the reactor blend composites their wear resistance even increases into the range of the monomodal UHMWPE reference. Herein, the all-PE composite 50RB63 which contained the highest content of 32 wt.-% UHMWPE showed the lowest wear rate of 2.4 ± 0.7 µm h^{-1}. The observed scatter of the wear rates arises from the scatter of the roughness of the steel rings and possibly from variations in the degree of orientation of the polymer specimens. Within the xxRB40 system

the beneficial role of the UHMWPE component on the wear resistance is clearly obvious when only the ratio of HDPE to RB40 is varied. The coefficient of friction was not significantly different, but the scatter could hide a minimal increased coefficient of friction for an increased wear resistance, which is a typical dependence for an overloaded thermoplastic system. The effect of the HDPE wax on the tribological performance is more complex as can be seen for 30RByy composites. When the ratio of UHMWPE to HDPE wax is varied, positive lubricating effects of the HDPE-wax are impaired by the weakening influence of high amounts of HDPE wax on the mechanical performance of the composites as can be found for 30RB50, 30RB63 and 50RByy. For these cases the coefficient of friction is significantly lower for an increased wear resistance, which is typical for a tribological loading when the thermoplast is able to withstand the attacking topography. In case of the composites when the wear rate clearly shows the beneficial role of the UHWMPE content an increased stiffness, increased strength and increased impact strength go along with an increased wear resistance.

Conclusions

Melt processing of HDPE with nanostructured bimodal UHMWPE/HDPE wax reactor blend (RB) additives affords thermoplastic all-PE single-component composites exhibiting simultaneous massive improvements of stiffness, strength, and toughness in conjunction with unprecedented high wear resistance similar to that of neat UHMWPE. These all-PE single-component composites are reinforced by extended-chain UHMWPE 1D nanostructures resembling nanofibers with average diameter of 100 nm, formed by flow-induced UHMWPE crystallization and verified by means of SEM imaging and DSC analysis. Since UHMWPE 1D nanostructures nucleate HDPE crystallization shish-kebab fiber-like structures are obtained. This UHMWPE 1D nanostructure formation does not involve either formation or handling of hazardous UHMWPE nanoparticles and takes place during injection molding of HDPE/RB melt blends. Nanostructure formation during RB synthesis and melt compounding

are prerequisite for all-PE-composite formation. On one hand, UHMWPE nanophase separation prevents entanglement accompanied by undesirable build-up of melt viscosity. On the other hand, opposite to micron-sized UHMWPE, UHMWPE nanostructures readily melt during short cycle times of melt processing producing nanostructured 1D UHMWPE reinforcing phases. Typically the bimodal RB intermediates contain up to 63 wt.-% nanophase-separated UHMWPE embedded in HDPE wax which serves as lubricant and processing aid lowering melt viscosity. RB additives are readily tailored by ethylene polymerization on supported two-site chromium catalysts. Whereas the RB addition to HDPE governs UHMWPE content of all-PE composites, the blend ratio of catalytic sites during RB preparation controls the UHMWPE/HDPE wax ratio. Hence melt compounding enables tailoring of trimodal all-PE composites with independently variable UHMWPE content at constant UHMWPE/HDPE wax weight ratio both of which are essential for improving all-PE composite melt processability and property profiles. All-PE composite self-reinforcement is primarily affected by the UHMWPE content. For instance at 32 wt.-% UHMWPE content, corresponding to 50 wt.-% of RB63 containing 63 wt.-% of UHMWPE, UHMWPE 1D nanostructure formation accounts for massive self-reinforcement as reflected by improved Young's modulus (+ 420%), tensile strength (+ 740%) and notched Izod impact strength (+ 650%) with respect to neat HDPE. For the first time, as verified by tribological investigations, tailored all-PE composites afford high wear resistance entering ranges typical for polyamide or monomodal UHMWPE which is not processable by injection molding under identical conditions. As a rule raising UHMWPE content of HDPE/RB blends is highly beneficial with respect to simultaneously improving wear resistance, stiffness, strength and toughness. At lower UHMWPE content, as observed in the cases of 30RB33 and 30RB40, the lubricating effect of built-in HDPE wax is likely to contribute to wear resistance. In conclusion, all-PE composite formation via melt compounding of RB with HDPE represents a versatile route for converting HDPE commodities into new generations of HDPE high

performance engineering thermoplastics exhibiting improved wear resistance similar to that of UHMWPE combined with attractive toughness/stiffness/strength balance but without sacrificing the attractive features of HDPE commodities such as low cost, high energy and resource efficiency, recycling and facile processing by injection molding, blow molding and extrusion. This approach of 1D nanostructure formation during melt processing using polymers with tailored molar mass distributions will stimulate the development of new generations of advanced sustainable all-polymer single-component composites which are of special interest for cyclic economy.

AUTHOR INFORMATION

Corresponding Author

* E-mail: rolfmuelhaupt@web.de

Author Contributions

The manuscript was written through contributions of all authors. All authors have given approval to the final version of the manuscript.

ACKNOWLEDGMENTS

The authors gratefully acknowledge the financial support by the Sustainability Center Freiburg. The authors are also grateful to Lyondellbasell Industries for long-term support in research on polymerization catalysis and self-reinforced polyethylene. We also would like to thank Rim Sayed Ahmad, Marina Hagios and Andreas Warmbold for assistance in polymerization catalysis and polymer characterization.

REFERENCES

(1) Sturzel, M.; Mihan, S.; Mulhaupt, R. From Multisite Polymerization Catalysis to Sustainable Materials and All-Polyolefin Composites. *Chemical reviews* **2016**, *116*, 1398–1433.

(2) Kurtz, S. M. *UHMWPE biomaterials handbook: ultra high molecular weight polyethylene in total joint replacement and medical devices*; Academic Press, 2009.

(3) Jordan, N.; Olley, R.; Bassett, D.; Hine, P.; Ward, I. The development of morphology during hot compaction of Tensylon high-modulus polyethylene tapes and woven cloths. *Polymer* **2002**, *43*, 3397–3404.

(4) Ward, I. M.; Hine, P. J. The science and technology of hot compaction. *Polymer* **2004**, *45*, 1413–1427.

(5) Deng, M.; Shalaby, S. W. Properties of self-reinforced ultra-high-molecular-weight polyethylene composites. *Biomaterials* **1997**, *18*, 645–655.

(6) Li, S. Ultra high molecular weight polyethylene: From charnley to cross-linked. *Operative Techniques in Orthopaedics* **2001**, *11*, 288–295.

(7) Capiati, N. J.; Porter, R. S. The concept of one polymer composites modelled with high density polyethylene. *J Mater Sci* **1975**, *10*, 1671–1677.

(8) Matabola, K. P.; Vries, A. R. de; Moolman, F. S.; Luyt, A. S. Single polymer composites: A review. *J Mater Sci* **2009**, *44*, 6213–6222.

(9) Kmetty, Á.; Bárány, T.; Karger-Kocsis, J. Self-reinforced polymeric materials: a review. *Progress in Polymer Science* **2010**, *35*, 1288–1310.

(10) Pope, D. P.; Keller, A. A study of the chain extending effect of elongational flow in polymer solutions. *Colloid and Polymer Science* **1978**, *256*, 751–756.

(11) Krumme, A.; Lehtinen, A.; Adamovsky, S.; Schick, C.; Roots, J.; Viikna, A. Crystallization behavior of some unimodal and bimodal linear low-density polyethylenes at moderate and high supercooling. *J. Polym. Sci. B Polym. Phys.* **2008**, *46*, 1577–1588.

(12) Boscoletto, A.; Franco, R.; Scapin, M.; Tavan, M. An investigation on rheological and impact behaviour of high density and ultra high molecular weight polyethylene mixtures. *European Polymer Journal* **1997**, *33*, 97–105.

(13) Kukalyekar, N.; Balzano, L.; Peters, G. W. M.; Rastogi, S.; Chadwick, J. C. Characteristics of Bimodal Polyethylene Prepared via Co-Immobilization of Chromium and Iron Catalysts on an MgCl2-Based Support. *Macromolecular Reaction Engineering* **2009**, *3*, 448–454.

(14) Tinçer, T.; Coşkun, M. Melt blending of ultra high molecular weight and high density polyethylene: The effect of mixing rate on thermal, mechanical, and morphological properties. *Polym Eng Sci* **1993**, *33*, 1243–1250.

(15) Diop, M. F.; Burghardt, W. R.; Torkelson, J. M. Well-mixed blends of HDPE and ultrahigh molecular weight polyethylene with major improvements in impact strength achieved via solid-state shear pulverization. *Polymer* **2014**, *55*, 4948–4958.

(16) Rastogi, S.; Yao, Y.; Ronca, S.; Bos, J.; van der Eem, J. Unprecedented High-Modulus High-Strength Tapes and Films of Ultrahigh Molecular Weight Polyethylene via Solvent-Free Route. *Macromolecules* **2011**, *44*, 5558–5568.

(17) Böhm, L. L. The ethylene polymerization with Ziegler catalysts: fifty years after the discovery. *Angewandte Chemie International Edition* **2003**, *42*, 5010–5030.

(18) Kurek, A.; Mark, S.; Enders, M.; Kristen, M. O.; Mülhaupt, R. Mesoporous silica supported multiple single-site catalysts and polyethylene reactor blends with tailor-made trimodal and ultra-broad molecular weight distributions. *Macromol. Rapid Commun.* **2010**, *31*, 1359–1363.

(19) Stürzel, M.; Hees, T.; Enders, M.; Thomann, Y.; Blattmann, H.; Mülhaupt, R. Nanostructured Polyethylene Reactor Blends with Tailored Trimodal Molar Mass Distributions as Melt-Processable All-Polymer Composites. *Macromolecules* **2016**, *49*, 8048–8060.
(20) Stürzel, M.; Kurek, A. G.; Hees, T.; Thomann, Y.; Blattmann, H.; Mülhaupt, R. Multisite catalyst mediated polymer nanostructure formation and self-reinforced polyethylene reactor blends with improved toughness/stiffness balance. *Polymer* **2016**, *102*, 112–118.
(21) Stürzel, M.; Thomann, Y.; Enders, M.; Mülhaupt, R. Graphene-supported dual-site catalysts for preparing self-reinforcing polyethylene reactor blends containing UHMWPE nanoplatelets and in situ UHMWPE shish-kebab nanofibers. *Macromolecules* **2014**, *47*, 4979–4986.
(22) Kurek, A.; Xalter, R.; Stürzel, M.; Mülhaupt, R. Silica Nanofoam (NF) supported single- and dual-site catalysts for ethylene polymerization with morphology control and tailored bimodal molar mass distributions. *Macromolecules* **2013**, *46*, 9197–9201.
(23) Hofmann, D.; Kurek, A.; Thomann, R.; Schwabe, J.; Mark, S.; Enders, M.; Hees, T.; Mülhaupt, R. Tailored Nanostructured HDPE Wax/UHMWPE Reactor Blends as Additives for Melt-Processable All-Polyethylene Composites and in Situ UHMWPE Fiber Reinforcement. *Macromolecules* **2017**, *50*, 8129–8139.
(24) Stürzel, M.; Kurek, A.; Anselm, M.; Halbach, T.; Mülhaupt, R. Polyolefin Nanocomposites and Hybrid Catalysts. In *Polyolefins: 50 years after Ziegler and Natta II: Polyolefins by Metallocenes and Other Single-Site Catalysts*; Kaminsky, W., Ed.; Springer Berlin Heidelberg: Berlin, Heidelberg, 2013; pp 279–309.
(25) Zhong, F.; Schwabe, J.; Hofmann, D.; Meier, J.; Thomann, R.; Enders, M.; Mülhaupt, R. All-polyethylene composites reinforced via extended-chain UHMWPE nanostructure formation during melt processing. *Polymer* **2018**, *140*, 107–116.
(26) Calvert, P. D.; Uhlmann, D. R. Direct crystallization of extended-chain crystals of polyethylene from the melt at high pressure. *J. Polym. Sci. B Polym. Lett.* **1970**, *8*, 165–172.
(27) Fischer, E. W.; Puderbach, H. Untersuchungen zur Ursache der Entstehung von "Extended Chain"-Kristallen des Polyäthylens. *Kolloid-Zeitschrift und Zeitschrift für Polymere* **1969**, *235*, 1260–1265.
(28) Briscoe, B. J.; Sinha, S. K. Wear of polymers. *Proceedings of the Institution of Mechanical Engineers, Part J: Journal of Engineering Tribology* **2002**, *216*, 401–413.
(29) Briscoe, B. J.; Sinha, S. K. Scratch Resistance and Localised Damage Characteristics of Polymer Surfaces – a Review. *Mat.-wiss. u. Werkstofftech.* **2003**, *34*, 989–1002.
(30) Abdel-Wahed, S. A.; Koplin, C.; Jaeger, R.; Scherge, M. On the Transition from Static to Dynamic Boundary Friction of Lubricated PEEK for a Spreading Adhesive Contact by Macroscopic Oscillatory Tribometry. *Lubricants* **2017**, *5*, 21.
(31) Shipway, P. H.; Ngao, N. K. Microscale abrasive wear of polymeric materials. *Wear* **2003**, *255*, 742–750.
(32) Samyn, P.; Schoukens, G. Calculation and significance of the maximum polymer surface temperature T* in reciprocating cylinder‐on‐plate sliding. *Polymer Engineering & Science* **2008**, *48*, 774–785.
(33) Menezes, P. L.; Kailas, S. V.; Lovell, M. R. Friction and transfer layer formation in polymer–steel tribo-system: role of surface texture and roughness parameters. *Wear* **2011**, *271*, 2213–2221.
(34) Bahadur, S. The development of transfer layers and their role in polymer tribology. *Wear* **2000**, *245*, 92–99.
(35) Scherge, M.; Kramlich, J.; Böttcher, R.; Hoppe, T. Running-in due to material transfer of lubricated steel/PA46 (aliphatic polyamide) contacts. *Wear* **2013**, *301*, 758–762.
(36) Viswanath, N.; Bellow, D. G. Development of an equation for the wear of polymers. *Wear* **1995**, *181*, 42–49.

(37) Scherge, M.; Linsler, D.; Schlarb, T. The running-in corridor of lubricated metal–metal contacts. *Wear* **2015**, *342*, 60–64.
(38) Shipway, P. H.; Ngao, N. K. Microscale abrasive wear of polymeric materials. *Wear* **2003**, *255*, 742–750.
(39) Budinski, K. G. Resistance to particle abrasion of selected plastics. *Wear* **1997**, *203*, 302–309.
(40) Unal, H.; Sen, U.; Mimaroglu, A. Dry sliding wear characteristics of some industrial polymers against steel counterface. *Tribology International* **2004**, *37*, 727–732.
(41) Wake, W. C. Tribologie der Polymere. H. Uetz and J. Wiedemeyer, Hanser, Munich and Vienna, 1984. pp. x+ 378, price DM198. 00. ISBN 3 ‐ 446 ‐ 14050 ‐ 6. *Polymer International* **1986**, *18*, 211–212.
(42) Zhang, A. Y.; Jisheng, E.; Allan, P. S.; Bevis, M. J. Enhancement in micro-fatigue resistance of UHMWPE and HDPE processed by SCORIM. *Journal of materials science* **2002**, *37*, 3189–3198.
(43) Lukens, W. W.; Yang, P.; Stucky, G. D. Synthesis of Mesocellular Silica Foams with Tunable Window and Cell Dimensions. *Chem. Mater.* **2001**, *13*, 28–34.
(44) Esteruelas, M. A.; Lopez, A. M.; Mendez, L.; Olivan, M.; Onate, E. Preparation, Structure, and Ethylene Polymerization Behavior of Bis(imino)pyridyl Chromium(III) Complexes. *Organometallics* **2003**, *22*, 395–406.
(45) Fernández, P.; Pritzkow, H.; Carbó, J. J.; Hofmann, P.; Enders, M. 1 H NMR Investigation of Paramagnetic Chromium(III) Olefin Polymerization Catalysts: Experimental Results, Shift Assignment and Prediction by Quantum Chemical Calculations †. *Organometallics* **2007**, *26*, 4402–4412.
(46) Enders, M.; Kohl, G.; Pritzkow, H. Synthesis of Main Group and Transition Metal Complexes with the (8-Quinolyl)cyclopentadienyl Ligand and Their Application in the Polymerization of Ethylene. *Organometallics* **2004**, *23*, 3832–3839.

TOC

1D-nanostructure formation during melt processing in the presence of tunable bimodal reactor blends affords all-PE single-component composites exhibiting simultaneously improved wear resistance, stiffness, strength, and toughness. Wear resistance similar to that of UHMWPE and high performance are achieved without addition of alien materials and without sacrificing other benefits typical for HDPE commodities.

Wear resistant all-PE single-component composites via 1D nanostructure formation during melt processing

Timo Hees, Fan Zhong, Christof Koplin, Raimund Jaeger, Rolf Mülhaupt*

ToC figure